Atmospheric
Chemistry
and Physics
Discussions

Open Access

On the link between hygroscopicity, volatility, and oxidation state of ambient and water-soluble aerosol in the Southeastern United States

K. M. Cerully[1,*], A. Bougiatioti[2,3], J. R. Hite Jr.[2], H. Guo[2], L. Xu[1], N. L. Ng[1,2], R. Weber[2], and A. Nenes[1,2,4]

[1]School of Chemical and Biomolecular Engineering, Georgia Institute of Technology, Atlanta, GA, USA
[2]School of Earth and Atmospheric Sciences, Georgia Institute of Technology, Atlanta, GA, USA
[3]Laser Remote Sensing Laboratory, National Technical University of Athens, Zografou, Greece
[4]Foundation for Research and Technology, Hellas, Patras, Greece
[*]now at: TSI, Inc., Shoreview, MN, USA

Title Page

Abstract	Introduction
Conclusions	References
Tables	Figures

|◄ | ►|
◄ | ►
Back | Close

Full Screen / Esc

Printer-friendly Version

Interactive Discussion

Abstract

The formation of secondary organic aerosol (SOA) combined with the partitioning of semi-volatile organic components can impact numerous aerosol properties including cloud condensation nuclei (CCN) activity, hygroscopicity and volatility. During the summer 2013 Southern Oxidant and Aerosol Study (SOAS) field campaign in a rural site in the Southeastern United States, a suite of instruments including a CCN counter, a thermodenuder (TD) and a high resolution time-of-flight aerosol mass spectrometer (AMS) were used to measure CCN activity, aerosol volatility, composition and oxidation state. Particles were either sampled directly from ambient or through a Particle Into Liquid Sampler (PILS), allowing the investigation of the water-soluble aerosol component. Ambient aerosol exhibited size-dependent composition with larger particles being more hygroscopic. The hygroscopicity of thermally-denuded aerosol was similar between ambient and PILS-generated aerosol and showed limited dependence on volatilization. Results of AMS 3-factor Positive Matrix Factorization (PMF) analysis for the PILS-generated aerosol showed that the most hygroscopic components are most likely the most and the least volatile features of the aerosol. No clear relationship was found between organic hygroscopicity and oxygen-to-carbon ratio; in fact, Isoprene organic aerosol (Isoprene-OA) was found to be the most hygroscopic factor, while at the same time being the least oxidized and likely most volatile of all PMF factors. Considering the diurnal variation of each PMF factor and its associated hygroscopicity, Isoprene-OA and More Oxidized – Oxidized Oxygenated Organic Aerosol (MO-OOA) are the prime contributors to hygroscopicity and covary with Less Oxidized – Oxidized Oxygenated Organic Aerosol (LO-OOA) in a way that induces the observed diurnal invariance in total organic hygroscopicity. Biomass Burning Organic Aerosol (BBOA) contributed little to aerosol hygroscopicity, which is expected since there was little biomass burning activity during the sampling period examined.

1 Introduction

Aerosol are well known to be important drivers of climate from regional to global scales by scattering and absorbing radiation (IPCC, 2007, 2013) as well as acting as cloud condensation nuclei (CCN). Though much progress has been made in understanding the role of aerosol in the climate system, the formation of secondary organic aerosol (SOA) and the partitioning of semi-volatile organics are topics subject to considerable uncertainty (e.g., Kanakidou et al., 2005; Goldstein and Galbally, 2007; Kroll and Seinfeld, 2008; Donahue et al., 2009; Hallquist et al., 2009; Ervens et al., 2011). Recent studies show that different estimation methods of SOA production result in ranges from 140 to 910 Tg C/yr (Goldstein and Galbally, 2007). The large uncertainty in these estimates (e.g., Pye and Seinfeld, 2010; Hallquist et al., 2009; Jimenez et al., 2009; Kanakidou et al., 2005) illustrates the need for better understanding of organic aerosol composition, volatility, hygroscopicity, and CCN activity.

Few studies have investigated the link between aerosol hygroscopicity, volatility, and level of aerosol oxidation (e.g., Jimenez et al., 2009; Poulain et al., 2010; Tritscher et al., 2011; Hong et al., 2013), though numerous studies have focused on the link between two of these parameters (e.g., Kuwata et al., 2007; Asa-Awuku et al., 2009; Meyer et al., 2009; Massoli et al., 2010; Chang et al., 2010; Lambe et al., 2011; Lathem et al., 2013; Frosch et al., 2011, 2013; Villani et al., 2013; Xu et al., 2014b). Several studies have shown and proposed parameterizations for the relationship between organic hygroscopicity and degree of oxidation (Chang et al., 2010; Massoli et al., 2010; Lambe et al., 2011; Frosch et al., 2013), with the hygroscopicity parameter, κ, being either inferred from subsaturated growth factor (GF) measurements or supersaturated CCN activation spectra (Petters and Kreidenweis, 2007), and the degree of oxidation represented by the oxygen to carbon ratio (O : C) or f_{44}, the ratio of the m/z 44 peak to the total organics signal in an aerosol mass spectrometer (AMS) (Ng et al., 2010; Aiken et al., 2008). Jimenez et al. (2009) showed results of several studies correlating GF with O : C and proposed a 2-dimensional framework for organic aerosol where

hygroscopicity and oxidation level increase with decreasing volatility. There are several other studies, though, that have shown that the link between these properties is not always straightforward (e.g., Meyer et al., 2009; Poulain et al., 2010; Frosch et al., 2011; Tritscher et al., 2011; Lathem et al., 2013; Alfarra et al., 2013; Villani et al., 2013).

Frosch et al. (2011) saw weak sensitivity of supersaturated κ to O : C and f_{44}, respectively; Alfarra et al. (2013) saw weak correlation for both subsaturated and supersaturated hygroscopicity measurements with f_{44} in laboratory studies of α-pinene SOA. Tritscher et al. (2011) found in chamber studies of α-pinene SOA that volatility generally decreased while subsaturated hygroscopicity and O : C remained fairly constant, and an additional study of α-pinene SOA by Meyer et al. (2009) measured a decrease in subsaturated hygroscopicity with increased volatility. Lathem et al. (2013) found that for biomass burning aerosol sampled during the ARCTAS and ARCPAC field campaigns, supersaturated organic hygroscopicity increased while O : C remained fairly constant. In ambient measurements by Villani et al. (2013), subsaturated hygroscopicity in several externally mixed air masses was found to both increase or decrease after volatilization. Asa-Awuku et al. (2009) observed that the most hygroscopic fraction of β-caryophyllene SOA was also the most volatile. Kuwata et al. (2007) found for subsaturated measurements of ambient aerosol in Tokyo that, after briefly heating to 400 °C, a less hygroscopic particle mode was also less volatile while a more hygroscopic mode was more volatile. The results of these studies illustrate the range of possible relationships between hygroscopicity, volatility, and oxidation level and the need to better understand why and when these interactions occur. An additional level of complexity arises in interpreting these results as subsaturated GF and supersaturated κ measurements can differ due to the difference in water volume between measurement conditions, thus impacting the assumption of an ideal solution and the importance of surface tension effects (Wex et al., 2009; Petters et al., 2009; Ruehl et al., 2010). Furthermore, recent studies have shown that average carbon oxidation state, $\overline{OS}_c$, may be a better indicator of aerosol oxidation than O : C as O : C may not capture oxidative changes due to the breaking and forming of bonds (Kroll et al., 2009, 2011).

Also important to SOA formation and processing are aqueous phase aerosol. Aqueous particles can both absorb species from the gas phase and serve as a medium for aqueous SOA production (Zuend and Seinfeld, 2012; Ervens et al., 2011, 2013; Sareen et al., 2013). Hennigan et al. (2009) found that water-soluble organic carbon represented a major portion of SOA in Atlanta. It has been proposed that SOA produced in the aqueous phase may have higher κ than SOA formed in the gas-phase with an upper limit comparable to ammonium sulfate ($\kappa = 0.6$) (Ervens et al., 2011); few experiments, however, have quantified the impact of SOA aqueous phase processes on total κ in ambient aerosol.

The Southeastern United States presents itself as a particularly interesting location of study, as it has experienced an overall cooling trend in surface temperature, in contrast to the warming trend seen elsewhere in the United States (Goldstein et al., 2009; Portmann et al., 2009). Carlton and Turpin (2013) found that aqueous SOA formation is particularly important in the eastern United States. These findings demonstrate that the SOA processes happening in this region are both complex and important. Motivated by these findings, the Southern Aerosol and Oxidant Study (SOAS) was a collaborative field mission which aimed to study the aerosol in the region. This study focuses on aerosol collected at a rural field site in Centreville, Alabama, and uses a variety of aerosol instrumentation to probe aerosol composition, volatility, and CCN properties.

2 Data collection

2.1 Measurement site

Data were collected during the Southern Oxidant and Aerosol Study (SOAS; http://soas2013.rutgers.edu), part of the Southeast Atmosphere Study (SAS; http://www.eol.ucar.edu/projects/sas), in Centreville, Alabama (+32°54′11.81″ N, 87°14′59″ W), a site highly influenced by biogenic VOC emissions combined with varying levels of anthropogenic influence (http://soas2013.rutgers.edu/). Measurements were taken

from 1 June through 15 July 2013, using a suite of aerosol instrumentation, including a Droplet Measurement Technologies Continuous-Flow Streamwise Thermal Gradient CCN counter (CFSTGC, referred to hereafter as the CCNc; Roberts and Nenes, 2005; Lance et al., 2006), thermodenuder (TD; Cerully et al., 2014), Particle-Into-Liquid-Sampler (PILS; Weber et al., 2001; Orsini et al., 2003), and high resolution time-of-flight aerosol mass spectrometer (HR-ToF-AMS, referred to hereafter as AMS; DeCarlo et al., 2006) to quantify CCN activity and hygroscopicity, volatility, water-soluble aerosol components, and aerosol composition and oxidation state, respectively. This study will primarily focus on comparing non-denuded and thermally-denuded measurements in order to investigate the relationship between hygroscopicity, volatility, and oxidation for both ambient and water-soluble ambient size-resolved and $PM_{1.0}$ aerosol.

2.2 Experimental setup and data collection

The instrument setup is shown in Fig. 1. Aerosol was collected using a $PM_{1.0}$ cyclone and either sampled directly from ambient or passed through the PILS; the water-soluble fraction of the ambient aerosol measured will be herafter referred to as PILS aerosol. For ambient sampling, aerosol was first dried using a Nafion dryer and charge-neutralized using a Po-210 bipolar charging source. For PILS sampling, aerosol were collected directly from ambient before being dried, thus any aqueous phase material in the ambient aerosol is also captured by the PILS. The PILS liquid is then filtered (25 mm diameter 0.45 μm pore syringe filter, Fisher Scientific, Fisherbrand*), nebulized (U-5000AT, Cetac Technologies Inc., Omaha, Nebraska, USA; Ohata et al., 2011), dried with a Nafion dryer, and charge-neutralized. The polydisperse aerosol stream then passed through the TD or through a bypass line before being sampled by the AMS, Scanning Mobility Particle Sizer (SMPS; TSI Classifier model 3080, Condensation Particle Counter (CPC) model 3022A), and CCNc. To account for nebulizer efficiency and any losses in the PILS-nebulizer system, sulfate measured by the PILS-AMS system was compared to ambient AMS sulfate and used as a scaling factor. The CCNc was operated in Scanning Flow CCN Analysis (SFCA) mode (Moore and Nenes, 2009),

scanning flow rate sinusoidally from 0.2 to $0.9\,L\,min^{-1}$ then back to $0.2\,L\,min^{-1}$ over 2 min, resulting in a CCN spectrum between 0.10 and 0.40 % supersaturation, s (see Sect. 3.1). The flow entering the CCNc was held constant at $1\,L\,min^{-1}$ using a laminar flow box and introduced to the CCN column as needed. The sheath to aerosol ratio in the CCNc was approximately 10 : 1. The top-to-bottom temperature difference in the CCN instrument was 6 °C. Temperature set points in the TD heating section were switched between 60, 80, or 100 °C. In this setup, the TD was operated without a cooling section, as recondensation of vapors is minimal at low ambient mass loadings characteristic of the conditions during this study (e.g., Cerully et al., 2014; Saleh et al., 2011). The SMPS was operated with a sheath flow rate of $3.0\,L\,min^{-1}$ and aerosol flow rate of $0.30\,L\,min^{-1}$ (10 : 1 ratio), with the CPC 3022A in low flow mode. Aerosol size distributions were collected every 3 min, scanning particle sizes from 14.6 to 685.4 nm. The AMS was operated in V mode (DeCarlo et al., 2006) with a data averaging time of 3 min. AMS measures mass concentrations of non-sea salt chloride, sulfate, nitrate, ammonium, and organics; refractory species (at 600 °C), including seasalt, black carbon, and crustal material, are not detected. Separate from this setup was an additional PILS coupled with an ion chromatograph (IC), referred to hereafter as the PILS-IC, which measured the ambient water-soluble Na^+, NH_4^+, K^+, Ca^{2+}, Mg^{2+}, Cl^-, NO_3^-, NO_2^-, SO_4^{2-} as well as acetate, formate, and oxalate every 20 min (Orsini et al., 2003).

The sampling schedule shown in Fig. 2 was designed to allow for automated measurements of ambient and water-soluble ambient aerosol. Thermally-denuded measurements were conducted from 20 June to 15 July. The temperature in the TD heating section was switched between 60 and 80 °C from 20 June to midday 30 June 2013 (Fig. 2, solid red line), and between 60 and 100 °C from evening 30 June through 15 July 2013 (Fig. 2, dashed line). SMPS distributions and AMS spectra sampled right before or after each switch between ambient/PILS sampling lines or between bypass and TD thermal processing were discarded. This leaves 3 SMPS scans and AMS samples per 15 min measurement interval. CCN properties (e.g., CCN concen-

tration as a function of s) were averaged when more than one SFCA scan occurred during a single SMPS sample. CCN spectra were smoothed by fitting CCN concentrations as a function of s. These fits were filtered for cases where flow rate fit parameter SDs are greater than $25\,\text{cm}^3\,\text{min}^{-1}$, resulting in a supersaturation uncertainty of approximately $\pm\,0.03\,\%$ (according to the calibration described in Sect. 3.1). The resulting CCN concentrations were compared with activation spectra predicted by applying Köhler theory (Köhler, 1936) to SMPS-measured concentrations under the assumption that the distributions had a κ of approximately 0.2–0.3, a general estimate of an aerosol population composed of organics and ammonium sulfate with equal volume fractions or slightly higher organic volume fraction than ammonium sulfate (see Sect. 3.3), as a filter to help identify irregularities in the data. All supersaturations in the instrument were corrected for supersaturation depletion from condensation of water vapor onto the activated CCN (see Sect. 3.1). Data were further filtered for days with measured precipitation $\geq 0.1\,\text{mm}$ (5 min resolution precipitation data provided by Atmospheric Research & Analysis, Inc.) and for any influences from non-representative local sources (e.g., diesel exhaust from truck deliveries to the sampling site). As flow, and therefore supersaturation, is scanned in the CCNc, spectra were divided into bins of s (%) $\pm 0.005\,\%$ and averaged within each bin.

3   Methodology

3.1   Instrument calibration and supersaturation depletion

The relationship between supersaturation and instantaneous flow rate was calibrated using the procedures of Moore and Nenes (2009). Briefly, ammonium sulfate solution is atomized, dried using two silica gel diffusion dryers and charge-neutralized using Po-210. The dried aerosol is then classified by a differential mobility analyzer (DMA; TSI model 3081 and split between a CPC, giving the total number of condensation nuclei (CN), and the CCNc. The activation ratio, or ratio of CCN to CN concentration, is plotted

against instantaneous flow rate and fit to a sigmoid function. The point where half of the total particles act as CCN corresponds to a "critical flow rate" and the instantaneous value of supersaturation corresponds to the known critical supersaturation, s_c, of the classified ammonium sulfate (Moore and Nenes, 2009). This relationship is determined for a range of classified ammonium sulfate particles, resulting in a calibration curve, in this case ranging from 0.10 to 0.40 %.

The calibration method described above was conducted with ammonium sulfate aerosol concentrations below 700 cm^{-3} in order to avoid water vapor depletion in the instrument (Lathem and Nenes, 2011). For measurements made throughout the study, supersaturation depletion in the CCNc column was accounted for using the correction found in Raatikainen et al. (2014); this typically has a negligible effect when sampling low ambient number concentrations but can be important when sampling from the PILS-nebulizer system (Fig. 1, green dashed line) where total aerosol number concentrations can reach as high as approximately 2.5×10^5 cm^{-3}.

3.2 Determining total aerosol hygroscopicity

Aerosol activate in the CCNc when their critical supersaturation, s_c, is greater than the instantaneous supersaturation (i.e., flow rate), s, in the CCNc column. This s_c corresponds to a critical diameter, $d_{p,c}$, above which all particles activate. These parameters are used to determine the aerosol hygroscopicity parameter, κ (Petters and Kreidenweis, 2007)

$$\kappa = \frac{4A^3}{27 d_{p,c}^3 s_c^2} \tag{1}$$

where $A = (4M_w \sigma_w)/(RT \rho_w)$, and M_w, σ_w, and ρ_w are the molar mass, surface tension, and density, respectively, of water at the average mid-column temperature, T, in the CCNc (305 K). R is the universal gas constant. The $d_{p,c}$ is obtained by matching the concentration of CCN activated at a given s (where $s = s_c$) with the backwards inte-

grated SMPS number distribution (thus, the corresponding size bin and $d_{p,c}$; Moore et al., 2011). This analysis method operates under the assumption that the aerosol are internally mixed (i.e., particles of a given size have similar composition) and that the size-dependent hygroscopicity does not vary enough to inhibit activation at larger sizes. In cases where ambient or thermally-denuded measurements are inhomogeneous, κ is most representative of particles with sizes near $d_{p,c}$.

3.2.1 Uncertainty in measured hygroscopicity

The uncertainty in the measured κ can be mainly attributed to uncertainties in the measured particle diameter and instrument supersaturation and can be described by

$$\Delta \kappa = \sqrt{\left(\frac{\partial \kappa}{\partial s}\Delta s\right)^2 + \left(\frac{\partial \kappa}{\partial d_p}\Delta d_p\right)^2} \tag{2}$$

where Δs and Δd_p are the instrument uncertainties in CCNc-measured supersaturation and DMA-measured diameter, respectively. Absolute uncertainty from CCNc supersaturation is estimated at $\pm 0.04\%$ (Moore et al., 2011) while DMA sizing uncertainty, based on the width of the DMA transfer function (Wang and Flagan, 1990) and the 10 : 1 sheath to aerosol flow ratio used in this study, is approximately 10 %. Average critical diameters of ambient aerosol of 83, 95, and 116 nm and measured at supersaturations of 0.40, 0.30, and 0.20 %, respectively, are reported and discussed in Sect. 4. Applying these values to Eq. (2) gives a $\Delta \kappa$ of 0.033, 0.053, and 0.097 for 0.40, 0.30, and 0.20 % supersaturation, respectively.

3.3 Inferring organic aerosol hygroscopicity

Total aerosol hygroscopicity can be expressed as a sum of contributions from each aerosol component

$$\kappa = \sum_j \varepsilon_j \kappa_j \tag{3}$$

where ε_j and κ_j are the volume fraction and hygroscopicity of species j, respectively (Petters and Kreidenweis, 2007). Using this rule, aerosol can be separated into its organic, org, and inorganic, inorg, contributions to the total, measured hygroscopicity, where

$$\kappa = \varepsilon_{\text{org}} \kappa_{\text{org}} + \varepsilon_{\text{inorg}} \kappa_{\text{inorg}}. \tag{4}$$

Measurements of particle composition, in this case, can come from either AMS or PILS-IC measurements. Using the five aerosol components measured by AMS, aerosol can be separated into its primarily inorganic ($[NH_4^+]$, $[SO_4^{2-}]$, $[Cl^-]$, and $[NO_3^-]$) and organic ($[\text{Org}]$) mass concentrations. A typical organic density of $1.4\,\text{g cm}^{-3}$ is assumed for volume calculations (e.g., Moore et al., 2011; Lathem et al., 2013). In order to better assess the properties of the inorganic aerosol, the partitioning of aerosol between sulfate species is evaluated (Nenes et al., 1998; Moore et al., 2011; Lathem et al., 2013). Using the molar ratio of ammonium ions to sulfate ions, R_{SO_4}, sulfate is determined to exist as a mixture of ammonium bisulfate and sulfuric acid for $R_{\text{SO}_4} < 1$, as ammonium sulfate and ammonium bisulfate for $1 < R_{\text{SO}_4} < 2$, or as ammonium sulfate for $R_{\text{SO}_4} > 2$. This method assumes that the relative contribution of nitrate (and will therefore exist mainly in the gas phase) and other inorganic cations (such as sodium) to the aerosol is minimal, which is the case here. Inorganic cations are not measured by the AMS, while nitrates are not present owing to the high acidity of the aerosol sampled (Guo et al., 2014). Once the species are determined, volume fractions are calculated using AMS mass fractions and the species densities and hygroscopicities

Title Page

Abstract | Introduction

Conclusions | References

Tables | Figures

◄ | ►

◄ | ►

Back | Close

Full Screen / Esc

Printer-friendly Version

Interactive Discussion

listed in Padró et al. (2010). For mixtures of more than one compound (i.e., for the $R_{SO_4} < 1$ or $1 < R_{SO_4} < 2$ cases), inorganic properties are calculated as the average of the individual component properties.

PILS-IC measurements can also be used to determine the inorganic and organic contributions to the aerosol. In this case, as measurements of Na^+ are included (Guo et al., 2014), it can be assessed whether the presence of these species can impact the predicted aerosol hygroscopicity. The speciation of the inorganic fraction of the aerosol becomes more complex, and the ISORROPIA II aerosol thermodynamic equilibrium model (Nenes et al., 1998; Fountoukis and Nenes, 2007) was employed to determine the speciation of inorganic compounds in the aerosol using the PILS-IC measurements. κ and density for each of the components were taken from Padró et al. (2010) when available. Otherwise, estimated intrinsic κ of Sullivan et al. (2009) were used with densities from Perry and Green (1984). As PILS-IC does not measure organic compounds, the AMS organic mass is used for calculation of volume fractions.

4 Results

The temporal variation of κ and AMS inorganic mass fraction for ambient and PILS water-soluble aerosol at $s = 0.40\%$ are shown in Fig. 3. All κ values for this study, as shown in Fig. 3, represent the average of all κ values measured within a given 15 min sampling period. Thermally-denuded measurements are indicated by the set point temperature which the aerosol were exposed to in the TD. Throughout the study, the trends in ambient and PILS κ are similar (not shown), though the magnitude can vary at different supersaturations as indicated in Table 1. Note that the SDs in κ in Table 1 for all conditions are typically very close to the $\Delta\kappa$ values calculated in Sect. 3.2.1; thus, it is expected that changes in the average reported κ are robust. PILS aerosol show a slightly larger average hygroscopicity than the ambient aerosol measured at both $s = 0.30\%$ and $s = 0.40\%$. The increase in hygroscopicity of ambient aerosol with decreasing supersaturation indicates that ambient particles have increasing hygroscopic-

ity with size; average $d_{p, c}$ for ambient non-denuded aerosol at 0.40, 0.30, and 0.20 % s are 83 ± 9, 95 ± 9, and 116 ± 11 nm, respectively. As the mixing in the PILS system results in a completely chemically homogeneous aerosol, as opposed to the ambient measurements, PILS aerosol hygroscopicity is relatively invariant with supersaturation (Table 1). As approximately 80 % of the ambient aerosol measured throughout this study were found to be water-soluble and PILS aerosol composition and hygroscopicity is dominated by the the mass and composition of the larger sampled aerosol sizes (Guo et al., 2014), it is expected that the PILS aerosol is also representative of the bulk ambient aerosol. As such, the ambient non-denuded aerosol hygroscopicity at the largest diameters (i.e., measured at $s = 0.20$ %) is similar to that of the measured PILS aerosol. The previous discussion makes it reasonable to assume that any additional aqueous processes taking place in the PILS sampler have a negligible impact on the overall aerosol hygroscopicity. This assumption will be tested throughout the following analysis by comparing the properties of ambient aerosol measured at $s = 0.20$ %, which is expected to be most representative of the bulk aerosol and AMS measurements, and PILS aerosol measured at $s = 0.40$ %.

4.1 κ of thermally denuded and non-denuded aerosol

Comparisons of the hygroscopicities of thermally-denuded, referred to hereafter simply as denuded, and non-denuded aerosol sampled directly from ambient and by PILS are shown in Fig. 4. The points shown are averages of measurements taken within each 15 min sampling period and represent only those points where denuded and non-denuded samples were collected directly before or after one another. It is expected that denuding aerosol would volatilize organics, thus the remaining aerosol would have an increased inorganic fraction and display higher hygroscopicity than its non-denuded counterpart. Denuded PILS aerosol show slightly higher hygroscopicity than the non-denuded aerosol, though these changes in κ are within 10 %. Thermally-denuded ambient aerosol, on the other hand, displays hygroscopicity similar to that of the non-denuded aerosol.

An unexpected result is that the ambient aerosol hygroscopicity does not change much, even when significant volatilization occurs. There are several potential reasons why this may occur. Here, it is discussed how changes in κ are related to possible composition changes taking place in the aerosol, such as a negligible loss of mass, volatilization of inorganic material, or higher volatility compounds having higher hygroscopicity, and to the chosen measurement method. Regarding the loss of mass in the aerosol, if aerosol is largely non-volatile at these temperatures, a change in hygroscopicity after being thermally denuded would not be expected; this is not the case here. Average ambient aerosol mass fractions remaining (MFR) calculated from AMS data and the average relative change in thermally-denuded hygroscopicity, κ_{TD}, vs. non-denuded hygroscopicity, κ_o, for ambient measurements at $s = 0.20\%$ and PILS measurements at $s = 0.40\%$ are shown in Table 2. Volatilization (by mass) reaches as high as approximately 35 % in the ambient aerosol and 55 % in the PILS aerosol. Note that the measured mass fractions remaining is not expected to be the same for the PILS and ambient aerosol due to general shifts in composition with size expected for ambient aerosol; however, the expected changes in κ, if ambient aerosol at $s = 0.20\%$ and PILS aerosol should be relatively similar. Indeed, relative changes in hygroscopicity are, on average, only 12 % for ambient mass losses of approximately 35 %. Villani et al. (2013) also found small changes in hygroscopicity for thermally-denuded aerosol, measuring changes in subsaturated hygroscopicity generally less than 5 % for thermally-denuded (from 70 to 100 °C) aerosol measured at four unique ambient environments. They also determined that denuded particles could display increased or decreased hygroscopicity, as seen here.

The magnitude of changes in κ is dependent on how mass is lost in the aerosol particles. Assuming that volatilization is mainly associated with organics, the change in hygroscopicity expected for the data, particularly at 80 and 100 °C for PILS and ambient data, should be notable. For example, according to the mixing rule in Eq. (4), if for a given particle composed of equal volumes of inorganic, assuming inorganic κ equals that of ammonium sulfate of 0.6 (Petters and Kreidenweis, 2007), and organic, assum-

ing organic κ of 0.2 (organic κ typically ranges from 0.1 to 0.3; Petters and Kreidenweis, 2007), measured κ would equal 0.4. If the same particles were denuded and the loss of organic mass resulted in a particle that is 80 % by volume inorganic and 20 % by volume organic, the resulting total κ would equal 0.52 (a 30 % increase in measured κ). One issue that makes this argument more complex is that, while it might be expected that a majority of the mass fraction lost would be from organics, it is also known that inorganic compounds (such as ammonium sulfate) can volatilize at the temperatures set in the thermodenuder. For example, ammonium sulfate aerosol has been found to volatilize at as low as 75 °C (Clarke, 1991; Burtscher et al., 2001; An et al., 2007), potentially decreasing the expected change in hygroscopicity after denuding. In our data, the fraction of the inorganic mass lost in the denuder, did not exhibit any temperature dependence between 30 and 100 °C, indicating that volatilization is not the main cause of this phenomenon.

An additional possibility for changes in κ to be suppressed even after loss of organic and inorganic materials is a decrease in the remaining organic hygroscopicity after denuding. Conventional thought suggests that the more volatile the organic compounds, the less aged and less hygroscopic they are (e.g., Jimenez et al., 2009). This implies that if the lowest hygroscopicity compounds are volatilized first, the remaining organic compounds should be of higher hygroscopicity. If volatilized organic material is actually of higher κ than the remaining organics (e.g., as seen by Asa-Awuku et al., 2009), a decrease in the hygroscopicity of the remaining organic could suppress changes seen in the total κ after denuding.

One final and necessary component in evaluating these results and their consequences on CCN activity is to consider the effects of ambient size-resolved composition. Regarding measurement methods, as described in Sect. 3.2, the critical dry diameter, $d_{p, c}$, is determined by matching the CCN concentration with the backwards-integrated SMPS size distribution. Thus, κ is expected to be most representative of aerosol with similar diameter to $d_{p, c}$. According to Eq. (1), $d_{p, c}$ at a given s will change if κ changes, as might be expected when volatilizing material in the denuder. For a mix-

ture that is chemically homogeneous with size, as is the PILS aerosol, a change in $d_{p, c}$ should not have an effect on κ (see Table 1). As the ambient aerosol display size-dependent composition (Table 1), changes in $d_{p, c}$ could potentially affect κ. Thus, it is difficult to probe the overall changes in chemistry of a given particle, but it is possible to look at how changes impact CCN activation at a given supersaturation. These changes in hygroscopicity for a given supersaturation are a measure of the importance of volatilization on CCN activity. Results reported in Table 2 clearly show that even with ambient mass losses of $\sim$ 35 %, the effect of volatility on κ, and thus CCN activity, is at most 10 %.

4.2   Inferred organic hygroscopicity

Organic hygroscopicity, κ_{org}, was inferred using composition measurements from PM_1 AMS and PILS-IC with ISORROPIA II and the methods described in Sect. 3.3 (Table 3). PILS-IC compositions were averaged over 1 h (i.e., spanning 2 periods of non-denuded PILS measurements in the PILS-AMS-CCNc setup). Using AMS composition and the total measured κ to infer κ_{org} shows that, the less volatile organic aerosol is also less hygroscopic. Though the SDs in κ_{org} are nearly as large as the average κ_{org} values (Table 3), the consistent trend between PILS and ambient aerosol, with the possible exception of ambient κ_{org} at 80 °C (where the highest SD is also seen), suggests that the most volatile fraction in the aerosol actually is of higher hygroscopicity than the less volatile material. Though this contradicts the conventional view that the most volatile aerosol components are the least hygroscopic, the change in hygroscopicity of only the organic fraction of the aerosol with volatility has not been studied in the ambient environment to the knowledge of these authors. Such behavior has been seen in chamber-generated aerosol (e.g., Asa-Awuku et al., 2009). It is possible that the least volatile fraction is also the least hygroscopic due to the presence of oligomers, high molecular weight compounds with low volatility and solubility – hence hygroscopicity (e.g., Ervens et al., 2011; Li et al., 2011; Sareen et al., 2010; Asa-Awuku et al., 2009; Reynolds et al., 2006; Varutbangkul et al., 2006; Baltensperger et al., 2005; VanReken

et al., 2005; Kalberer et al., 2004). As temperature is increased in the thermodenuder, oligomers may partially dissociate into more volatile and hygroscopic fragments upon heating, contributing to the decreased hygroscopicity at increased temperatures in the TD (Table 3).

⁵ To evaluate the importance of assumptions of the inorganic composition in inferring the organic hygroscopicity, κ_{org} was additionally determined for non-denuded PILS aerosol using data from a PILS-IC system concurrently sampling non-denuded ambient aerosol and located separately from the main PILS-CCNc-AMS setup. Data were input to the ISORROPIA II aerosol equilibrium model to determine speciated composition of ¹⁰ the inorganics, investigating how realistic the assumptions are of treating the inorganic hygroscopicity as an ammonium and sulfate system only (Sect. 3.3). ISORROPIA II is able to resolve sodium, ammonium, magnesium, calcium, and potassium species. In Centerville, however, sodium, magnesium, calcium, and potassium components were found to typically be negligible. For this reason, there should be little difference in the ¹⁵ assumed inorganic hygroscopicity using the AMS or PILS-IC analysis methods. The slight decrease in PILS κ_{org} (~ 0.03; Table 3) resulting from PILS-IC vs. AMS analysis confirm the validity of using simplified assumptions of aerosol speciation to calculate inorganic hygroscopicity for this study and does not change the trend of decreased κ_{org} with increased volatility seen here.

²⁰ ## 4.3 Organic aerosol hygroscopicity and degree of oxidation

The potential link between organic hygroscopicity and the level of aerosol oxidation is investigated using AMS measurements of the bulk O : C ratio with the κ_{org} determined in Sect. 4.2 with. O : C throughout the study and for different TD sampling temperatures varied slightly with ambient average O : C values of 0.58 ± 0.06 for non-denuded ²⁵ aerosol; no variation in average O : C was seen for denuded aerosol, being 0.59 ± 0.05, 0.57 ± 0.04, and 0.59 ± 0.06 for TD temps of 60, 80, and 100 °C, respectively (Fig. 5, left). PILS- generated aerosol showed similar O : C values of 0.55 ± 0.04, 0.57 ± 0.05, 0.56 ± 0.03, and 0.53 ± 0.07 for non-denuded and denuded aerosol at 60, 80, and

Title Page

Abstract | Introduction

Conclusions | References

Tables | Figures

|◄ | ►|

◄ | ►

Back | Close

Full Screen / Esc

Printer-friendly Version

Interactive Discussion

100 °C, respectively (Fig. 5, right). There is no clear relationship between κ_{org} with O : C for any of this data as the correlation between κ_{org} and O : C in all cases is low ($R^2 < 0.23$ for ambient and < 0.53 for PILS aerosol).

The relationship between κ_{org} with average carbon oxidation state $\overline{OS}_c$, calculated as $2 \times$ O : C-H : C (where H : C is the hydrogen to carbon ratio of the aerosol measured by the AMS) is further investigated for the ambient aerosol (Fig. 6, left panel). While there is no clear relationship between κ_{org} and oxidation in terms of $\overline{OS}_c$, it appears that denuded aerosol at 100 °C are more oxidized than at other temperatures as might be expected, but not indicated by O : C. Measurements at 80 °C, though, still appear to be less oxidized than thermally-denuded at 60 °C. Although at first this seems counterintuitive (Sect. 2.2 and Figs. 2 and 3), 60 °C measurements were taken throughout the measurement period while 80 °C were taken only during the beginning portion of the study and 100 °C only during the latter portion of the study. Therefore, it is more appropriate to focus on the relationship between κ_{org} and $\overline{OS}_c$ for each separate measurement period (Fig. 6, right). In this case, $\overline{OS}_c$ is consistent with expectation that oxidation increases as more material is volatilized in the denuder as indicated by the change in $\overline{OS}_c$ between non-denuded, 60, and 100 °C measurements (Fig. 6, right, bottom) with comparable increases in $\overline{OS}_c$ for 60 and 80 °C measurements compared to non-denuded measurements (Fig. 6, right, top). This is not, however, the case for O : C, as O : C of 60 °C measurements remains greater than that of 100 °C measurements (not shown). O : C of 60, 80 °C, and non-denuded measurements are comparable (not shown). Overall, $\overline{OS}_c$ appears to be more consistent with the expectation of the least volatile fraction being the most oxidized while O : C appears to show no correlation with volatilization. Even $\overline{OS}_c$, however, may appear counter to expectation during portions of the sampling period (Fig. 6, left); this is a result of changing air masses which can change the relationship between hygroscopicity and volatility with oxidation. Further-

Hygroscopicity, volatility and oxidation state of aerosol in the SE United States

K. M. Cerully et al.

Title Page

Abstract	Introduction
Conclusions	References
Tables	Figures

|◄ | ►|

◄ | ►

Back | Close

Full Screen / Esc

Printer-friendly Version

Interactive Discussion

more, the increase in $\overline{OS}_c$ with volatility is still consistent with the potential presence of oligomers discussed in Sect. 4.2.

4.4 Attributing organic hygroscopicity to AMS factors

Positive Matrix Factorization (PMF; Lanz et al., 2007) analysis is performed on high-resolution organics mass spectra for source apportionment. A detailed discussion of the PMF results can be found in Xu et al. (2014a). In brief, four subtypes of OA are identified in the ambient aerosol after carefully examining the scaled residual, solution rotational ambiguity, and factor correlations with external tracers. Two oxygenated OA factors with high but differing O : C ratios are termed as more-oxidized OOA (MO-OOA, O : C = 0.8) and Less-oxidized OOA (LO-OOA, O : C = 0.46). MO-OOA contributes 39 % of total OA. LO-OOA, accounting for 32 % of OA, is found to be mainly from β-pinene oxidation by NO_3 radical. Biomass Burning OA (BBOA) factor, characterized by ions at m/z 60 ($C_2H_4O_2^+$) and 73 ($C_3H_5O_2^+$) in the mass spectrum, shows good correlation ($R = 0.8$) in time series with brown carbon. The fourth factor is interpreted as Isoprene-derived OA (Isoprene-OA). This factor exhibits a similar mass spectrum to laboratory-generated isoprene SOA via the reactive uptake of epoxydiols (prominent signals at $C_4H_5^+$ and $C_5H_6O^+$) (Lin et al., 2012; Nguyen et al., 2014). Additionally, it shows a good correlation with particle-phase methyltetrols (tracer for isoprene OA). PMF on the PILS aerosol resulted in 3 factors corresponding to LO-OOA, MO-OOA and Isoprene-OA; this is because during the period of measurements with the PILS, the concentration of BBOA was too low to expect a PMF factor to emerge from the analysis. PMF factors of the total PILS aerosol measured by AMS were used to perform linear regression on the PILS non-denuded κ_{org} (at $s = 0.40$ %) to infer the hygroscopicity of each PMF factor, and its contribution, to organic aerosol hygroscopicity:

$$\kappa_{org} = \varepsilon_{LO\text{-}OOA}\kappa_{LO\text{-}OOA} + \varepsilon_{MO\text{-}OOA}\kappa_{MO\text{-}OOA} + \varepsilon_{Isoprene\text{-}OA}\kappa_{Isoprene\text{-}OA} \qquad (5)$$

where properties are representative of AMS mass spectra for LO-OOA, MO-OOA and Isoprene-OA, respectively. A system of equations is determined using corresponding measurements of the PILS non-denuded κ_{org} and PMF factor mass fractions. A bootstrapped resampling of the regression indicates that while the average κ_{MO-OOA} and

5 $\kappa_{Isoprene-OA}$ are similar at 0.16 ± 0.02 and 0.20 ± 0.02, respectively, they are at least twice as large as the average κ_{LO-OOA} of 0.08 ± 0.02 (Fig. 7).

As a consistency check, the values of hygroscopicity parameter determined in Fig. 7 are compared against those retrieved from ambient κ_{org} measurements. Given that PILS-derived κ_{org} does not contain biomass burning aerosol, and, the method works

10 best for aerosol that is chemically uniform with size (e.g., Cerully et al., 2011), we analyze ambient data during periods where PILS data is available and for which the biomass burning factor in the ambient aerosol was less than 1 % of the total organic aerosol. This constraint filtered out periods of data for when the aerosol was an external mixture, as the aerosol was unimodal (not shown), and more consistent with

15 the requirement of chemical uniformity. The filtered data was then processed to infer the κ_{org} by application of Eq. (5). A subsequent bootstrap analysis lead to values of the hygroscopicity parameter that were very similar to those shown in Fig. 7: $\kappa_{Isoprene-OA} = 0.26 \pm 0.07; \kappa_{MO-OOA} = 0.17 \pm 0.05; \kappa_{LO-OOA} = 0.1 \pm 0.03$. The broader SDs of the ambient factor analysis are a consequence of the inherently larger uncertainty

20 associated with ambient aerosol analysis; nevertheless the analysis indicates that isoprene-OA is the most hygroscopic factor, followed by MO-OOA and LO-OOA.

O : C values of the MO-OOA, LO-OOA, and Isoprene-OA factors were determined to be 0.73, 0.47, and 0.41, respectively (Fig. 7) by following the procedure in Aiken et al. (2008). MO-OOA displays a higher κ_{org} and O : C compared to LO-OOA, but κ_{org}

25 does not clearly correlate with O : C for all three factors. It is difficult to determine why Isoprene-OA displays the lowest O : C and the highest value of κ_{org}, though this topic presents itself as an interesting area of future study. The results of O : C with κ_{org} of each PMF factor are comparable to that of $\overline{OS_c}$ with each factor κ_{org} (not shown).

From the average diurnal profile of the AMS mass factors (Fig. 8a) and the hygroscopicity parameter of each, one can then attribute the contribution of each factor to the overall κ_{org}. This is important, because it indicates the origin of aerosol hygrosocpicity throughout the day. Given that the biomass burning burning factor constituted roughly 10 % of the mass of the aerosol during the period sampled by the PILS, its contribution to total κ_{org} is small, but not negligible. We therefore determine an optimal estimate of its hygroscopicity, κ_{BB-OA}, by least squares fitting of the ambient κ_{org} for the whole sampling period to predictions using the PMF factors mass fractions and the mean values of $\kappa_{Isoprene-OA}$, κ_{MO-OOA} and κ_{LO-OOA} shown in Fig. 7; we find that $\kappa_{BB-OA} = 0.31$, which is at the upper limit of hygroscopicity observed from biomass burning samples (e.g., Asa-Awuku et. al., 2008). Based on this set of hygroscopicity parameters and the mass fractions presented in Fig. 8a, we then can determine the contribution of each mass factor to κ_{org}, and the resulting diurnal profile of κ_{org} all of which is shown in Fig. 8b. From the results it is clear that 40–60 % of the organic hygroscopicity originates from LO-OOA, and another 20–30 % from Isoprene-OA. The relatively low hygroscopicity of LO-OOA and its opposing diurnal cycle with respect to MO-OOA works synergistically with LO-OOA and Isoprene-OA to yield the relative invariance of κ_{org} with time of day. Biomass burning has a minor 10–15 % contribution to κ_{org}; given that the value of κ_{BB-OA} highly unlikely to go above 0.3, this constitutes an upper limit of BBOA contribution to hygroscopicity.

5   Conclusions

The volatility, hygroscopicity, and oxidation state of ambient and water-soluble ambient aerosol collected in a rural site in the Southeastern United States during the SOAS field campaign were investigated. κ measured at 0.40, 0.30, and 0.20 % supersaturation indicated that ambient aerosol exhibited size-dependent composition. Average κ at $s = 0.20$ % for thermally-denuded and non-denuded ambient aerosol display a strong similarity with PILS-generated aerosol at all supersaturations; κ of PILS aerosol at

$s = 0.40\%$ and ambient aerosol at $s = 0.20\%$ were compared and found to be remarkably similar throughout the study period, suggesting that the PILS aerosol were representative of the PM$_1$ average composition.

κ of thermally-denuded aerosol at 60, 80, and 100 °C showed similar results for both ambient and PILS-generated aerosol with κ increasing slightly with temperature and showing a much weaker dependence on volatilization than expected. Even after volatilizing $\sim 35\%$ of the ambient aerosol mass, relative changes in κ for PILS-generated and ambient aerosol are only approximately 12 %. If this finding is representative of other locations, this could mean that changes in volatility may be of minor significance in the case of bulk aerosol hygroscopic properties.

The hygroscopicity of the organic fraction, κ_{org}, remaining in the aerosol after volatilization was found to decrease slightly, which is against conventional thinking that the highest volatility compounds are the least hygroscopic. This trend has been observed previously in the laboratory (e.g., Asa-Awuku et al., 2009) and could be attributed to the presence of oligomers in the aerosol that dissociate into more volatile and more hygroscopic fragments upon heating. The least volatile aerosol did appear to be the most oxidized, as expected. This however, was only indicated by $\overline{\text{OS}}_{\text{c}}$, while no clear correlation was seen between O : C with volatility or hygroscopicity, consistent with the notion that $\overline{\text{OS}}_{\text{c}}$ a preferred indicator of oxidation (Kroll et al., 2011). Results of AMS 3-factor PMF analysis for the PILS aerosol were used to attribute the organic hygroscopicity of each PMF factor to the total κ_{org}. $\kappa_{\text{MO-OOA}}$ and $\kappa_{\text{Isoprene-OA}}$ showed the largest hygroscopicities of 0.16 ± 0.02 and 0.20 ± 0.02, respectively, and $\kappa_{\text{LO-OOA}}$ showed a two-fold lower hygroscopicity of 0.08 ± 0.02. These parameters were verified against independent hygroscopicity retreivals for the ambient aerosol during periods where the contribution of biomass burning was negligible. No clear relationship between organic hygroscopicity and O : C was found for all factors, particularly as O : C in this study varies only slightly (average O : C of non-denuded and thermally-denuded ambient measurements range from only 0.59 ± 0.05 to 0.57 ± 0.04). The hygroscopicity and O : C of MO-OOA, however, were greater than that of LO-OOA, consistent with

Title Page

Abstract | Introduction

Conclusions | References

Tables | Figures

|◄ | ►|

◄ | ►

Back | Close

Full Screen / Esc

Printer-friendly Version

Interactive Discussion

expectations. However, Isoprene-OA was found to be the most hygroscopic factor and was also the least oxidized (and likely the most volatile), which goes against expectations. Similar results were found when compared to $\overline{OS}_c$ as an indicator of aerosol oxidation.

5   Some important implications arise from this study. First, for the range of hygroscopicities measured, although still within the reported ranges (0.08–0.2) for organic aerosol, the most hygroscopic components are likely the most and least volatile features of the aerosol. This leads to a relative invariance in organic aerosol properties, as both local production and long range transport of organics can equally contribute to water 10 uptake, hence the climate forcing associated with organic aerosol. Wet-processing of the aerosol by generating new particles from the ambient soluble material collected in the PILS does not result in fundamentally different aerosol properties from those determined in the ambient aerosol, which means that deliquescence/efflorescence of aerosol in clouds does not alter the aerosol the hygroscopic properties of each organic 15 aerosol factor. Volatilization of the aerosol also does not appreciably affect its hygroscopicity, implying that semivolatile partitioning during dilution from boundary layer expansion, transport away from source region and entrainment into the free troposphere primarily affects organic aerosol mass and not its water uptake properties. Considering the diurnal variation of each PMF factor and its associated hygroscopicity, Isoprene-OA 20 and MO-OOA are the prime contributors to hygroscopicity and covary with LO-OOA in a way that induces the observed diurnal cycle in oganic hygroscopicity. BB-OA contributes here a minor role in aerosol hygroscopicity, which is expected since there was little biomass burning activity during the sampling period examined.

References

Aiken, A. C., DeCarlo, P. F., Kroll, J. H., Worsnop, D. R., Huffman, J. A., Docherty, K., Ulbrich, I. M., Mohr, C., Kimmel, J. R., Sueper, D., Zhang, Q., Sun, Y., Trimborn, A., Northway, M., Ziemann, P. J., Canagaratna, M. R., Onasch, T. B., Alfarra, R., Prevot, A. S. H., Dommen, J., Duplissy, J., Metzger, A., Baltensperger, U., and Jimenez, J. L.: O/C and OM/OC ratios of primary, secondary, and ambient organic aerosols with high-resolution time-of-flight aerosol mass spectrometry, Environ. Sci. Technol., 42, 4478–4485, 2008.

Alfarra, M. R., Good, N., Wyche, K. P., Hamilton, J. F., Monks, P. S., Lewis, A. C., and McFiggans, G.: Water uptake is independent of the inferred composition of secondary aerosols derived from multiple biogenic VOCs, Atmos. Chem. Phys., 13, 11769–11789, doi:10.5194/acp-13-11769-2013, 2013.

An, W. J., Pathak, R. K., Lee, B. H., and Pandis, S. N.: Aerosol volatility measurement using an improved thermodenuder: application to secondary organic aerosol, J. Aerosol Sci., 48, 305–314, doi:10.1016/j.jaerosci.2006.12.002, 2007.

Asa-Awuku, A., Sullivan, A. P., Hennigan, C. J., Weber, R. J., and Nenes, A.: Investigation of molar volume and surfactant characteristics of water-soluble organic compounds in biomass burning aerosol, Atmos. Chem. Phys., 8, 799–812, doi:10.5194/acp-8-799-2008, 2008.

Asa-Awuku, A., Engelhart, G. J., Lee, B. H., Pandis, S. N., and Nenes, A.: Relating CCN activity, volatility, and droplet growth kinetics of β-caryophyllene secondary organic aerosol, Atmos. Chem. Phys., 9, 795–812, doi:10.5194/acp-9-795-2009, 2009.

Baltensperger, U., Kalberer, M., Dommen, J., Paulsen, D., Alfarra, M. R., Coe, H., Fisseha, R., Gascho, A., Gysel, M., Nyeki, S., Sax, M., Steinbacher, M., Prevot, A. S. H., Sjögren, S., Weingartner, E., and Zenobi, R.: Secondary organic aerosols from anthropogenic and biogenic precursors, Faraday Discuss., 130, 265, doi:10.1039/B417367H, 2005.

Burtscher, H., Baltensperger, U., Bukowiecki, N., Cohn, P., Hüglin, C., Mohr, M., Matter, U., Nyeki, S., Schmatloch, V., Streit, N., and Weingartner, E.: Separation of volatile and non-

Title Page

Abstract	Introduction
Conclusions	References
Tables	Figures

|◄ | ►|
◄ | ►

Back | Close

Full Screen / Esc

Printer-friendly Version

Interactive Discussion

volatile aerosol fractions by thermodesorption: instrumental development and applications, J. Aerosol Sci., 32, 427–442, doi:10.1016/S0021-8502(00)00089-6, 2001.

Carlton, A. G. and Turpin, B. J.: Particle partitioning potential of organic compounds is highest in the Eastern US and driven by anthropogenic water, Atmos. Chem. Phys., 13, 10203–10214, doi:10.5194/acp-13-10203-2013, 2013.

Cerully, K. M., Raatikainen, T., Lance, S., Tkacik, D., Tiitta, P., Petäjä, T., Ehn, M., Kulmala, M., Worsnop, D. R., Laaksonen, A., Smith, J. N., and Nenes, A.: Aerosol hygroscopicity and CCN activation kinetics in a boreal forest environment during the 2007 EUCAARI campaign, Atmos. Chem. Phys., 11, 12369–12386, doi:10.5194/acp-11-12369-2011, 2011.

Cerully, K., Hite, J., McLaughlin, M., and Nenes, A.: Towards the determination of joint volatility-hygroscopicity distributions: instrument development and response characterization for single-component Aerosol, Aerosol. Sci. Tech., 48, 295–311, doi:, 2014.

Chang, R. Y.-W., Slowik, J. G., Shantz, N. C., Vlasenko, A., Liggio, J., Sjostedt, S. J., Leaitch, W. R., and Abbatt, J. P. D.: The hygroscopicity parameter (κ) of ambient organic aerosol at a field site subject to biogenic and anthropogenic influences: relationship to degree of aerosol oxidation, Atmos. Chem. Phys., 10, 5047–5064, doi:10.5194/acp-10-5047-2010, 2010.

Clarke, A. D.: A thermo-optic technique for in-situ analysis of size-resolved aerosol physico-chemistry, Atmos. Environ., 25, 635–644, doi:10.1016/0960-1686(91)90061-B, 1991.

DeCarlo, P. F., Kimmel, J. R., Trimborn, A., Northway, M. J., Jayne, J. T., Aiken, A. C., Gonin, M., Fuhrer, K., Horvath, T., Docherty, K. S., Worsnop, D. R., and Jimenez, J. L.: Field-deployable, high-resolution, time-of-flight aerosol mass spectrometer, Anal. Chem., 78, 8281–8289, doi:10.1021/ac061249n, 2006.

Donahue, N. M., Robinson, A. L., and Pandis, S. N.: Atmospheric organic particulate matter: from smoke to secondary organic aerosol, Atmos. Environ., 43, 94–106, doi:10.1016/j.atmosenv.2008.09.055, 2009.

Ervens, B., Turpin, B. J., and Weber, R. J.: Secondary organic aerosol formation in cloud droplets and aqueous particles (aqSOA): a review of laboratory, field and model studies, Atmos. Chem. Phys., 11, 11069–11102, doi:10.5194/acp-11-11069-2011, 2011.

Ervens, B., Wang, Y., Eagar, J., Leaitch, W. R., Macdonald, A. M., Valsaraj, K. T., and Herckes, P.: Dissolved organic carbon (DOC) and select aldehydes in cloud and fog water: the role of the aqueous phase in impacting trace gas budgets, Atmos. Chem. Phys., 13, 5117–5135, doi:10.5194/acp-13-5117-2013, 2013.

Title Page

Abstract	Introduction
Conclusions	References
Tables	Figures

|◄ | ►|

◄ | ►

Back | Close

Full Screen / Esc

Printer-friendly Version

Interactive Discussion

Fountoukis, C. and Nenes, A.: ISORROPIA II: a computationally efficient thermodynamic equilibrium model for K^+–Ca^{2+}–Mg^{2+}–NH_4^+–Na^+–SO_4^{2-}–NO_3^-–Cl^-–H_2O aerosols, Atmos. Chem. Phys., 7, 4639–4659, doi:10.5194/acp-7-4639-2007, 2007.

Frosch, M., Bilde, M., DeCarlo, P. F., Jurányi, Z., Tritscher, T., Dommen, J., Donahue, N. M., Gysel, M., Weingartner, E., and Baltensperger, U.: Relating cloud condensation nuclei activity and oxidation level of α-pinene secondary organic aerosols, J. Geophys. Res., 116, D2212, doi:, 2011.

Frosch, M., Bilde, M., Nenes, A., Praplan, A. P., Jurányi, Z., Dommen, J., Gysel, M., Weingartner, E., and Baltensperger, U.: CCN activity and volatility of β-caryophyllene secondary organic aerosol, Atmos. Chem. Phys., 13, 2283–2297, doi:10.5194/acp-13-2283-2013, 2013.

Goldstein, A. H. and Galbally, I. E.: Known and unexplored organic constituents in the Earth's atmosphere, Environ. Sci. Tech., 5, 1514–1521, doi:10.1021/es072476p, 2007.

Guo, H., Xu, L., Bougiatioti, A., Cerully, K. M., Capps, S. L., Hite, J. R., Carlton, A. G., Lee, S.-H., Bergin, M. H., Ng, N. L., Nenes, A., and Weber, R. J.: Particle water and pH in the southeastern United States, Atmos. Chem. Phys. Discuss., 14, 27143–27193, doi:10.5194/acpd-14-27143-2014, 2014.

Hallquist, M., Wenger, J. C., Baltensperger, U., Rudich, Y., Simpson, D., Claeys, M., Dommen, J., Donahue, N. M., George, C., Goldstein, A. H., Hamilton, J. F., Herrmann, H., Hoffmann, T., Iinuma, Y., Jang, M., Jenkin, M. E., Jimenez, J. L., Kiendler-Scharr, A., Maenhaut, W., McFiggans, G., Mentel, Th. F., Monod, A., Prévôt, A. S. H., Seinfeld, J. H., Surratt, J. D., Szmigielski, R., and Wildt, J.: The formation, properties and impact of secondary organic aerosol: current and emerging issues, Atmos. Chem. Phys., 9, 5155–5236, doi:10.5194/acp-9-5155-2009, 2009.

Hennigan, C. J., Bergin, M. H., Russell, A. G., Nenes, A., and Weber, R. J.: Gas/particle partitioning of water-soluble organic aerosol in Atlanta, Atmos. Chem. Phys., 9, 3613–3628, doi:10.5194/acp-9-3613-2009, 2009.

Hong, J., Häkkinen, S. A. K., Paramonov, M., Äijälä, M., Hakala, J., Nieminen, T., Mikkilä, J., Prisle, N. L., Kulmala, M., Riipinen, I., Bilde, M., Kerminen, V.-M., and Petäjä, T.: Hygroscopicity, CCN and volatility properties of submicron atmospheric aerosol in a boreal forest environment during the summer of 2010, Atmos. Chem. Phys., 14, 4733–4748, doi:10.5194/acp-14-4733-2014, 2014.

Title Page

Abstract	Introduction
Conclusions	References
Tables	Figures

◄	►
◄	►
Back	Close

Full Screen / Esc

Printer-friendly Version

Interactive Discussion

Intergovernmental Panel on Climate Change (IPCC): Climate Change 2007: The Physical Science Basis, Summary for Policymakers, available at: http://www.ipcc.ch/publications_and_data/ar4/syr/en/contents.html, 2007.

Intergovernmental Panel on Climate Change (IPCC): Climate Change 2013: The Physical Science Basis, Summary for Policymakers, available at: http://www.ipcc.ch/report/ar5/wg1/, 2013.

Jimenez, J. L., Canagaratna, M. R., Donahue, N. M., Prevot, A. S. H., Zhang, Q., Kroll, J. H., DeCarlo, P. F., Allan, J. D., Coe, H., Ng, N. L., Aiken, A. C., Docherty, K. S., Ulbrich, I. M., Grieshop, A. P., Robinson, A. L., Duplissy, J., Smith, J. D., Wilson, K. R., Lanz, V. A., Hueglin, C., Sun, Y. L., Tian, J., Laaksonen, A., Raatikainen, T., Rautiainen, J., Vaattovaara, P., Ehn, M., Kulmala, M., Tomlinson, J. M., Collins, D. R., Cubison, M. J., Dunlea, E. J., Huffman, J. A., Onasch, T. B., Alfarra, M. R., Williams, P. I., Bower, K., Kondo, Y., Schneider, J., Drewnick, F., Borrmann, S., Weimer, S., Demerjian, K., Salcedo, D., Cottrell, L., Griffin, R., Takami, A., Miyoshi, T., Hatakeyama, S., Shimono, A., Sun, J. Y., Zhang, Y. M., Dzepina, K., Kimmel, J. R., Sueper, D., Jayne, J. T., Herndon, S. C., Trimborn, A. M., Williams, L. R., Wood, E. C., Middlebrook, A. M., Kolb, C. E., Baltensperger, U., and Worsnop, D. R.: Evolution of organic aerosols in the atmosphere, Science, 326, 1525–1529, doi:10.1126/science.1180353, 2009.

Kalberer, M., Paulsen, D., Sax, M., Steinbacher, M., Dommen, J., Prevot, A. S. H., Fisseha, R., Weingartner, E., Frankevich, V., Zenobi, R., and Baltensperger, U.: Identification of polymers as major components of atmospheric organic aerosols, Science, 303, 1659–1662, doi:10.1126/science.1092185, 2004.

Kanakidou, M., Seinfeld, J. H., Pandis, S. N., Barnes, I., Dentener, F. J., Facchini, M. C., Van Dingenen, R., Ervens, B., Nenes, A., Nielsen, C. J., Swietlicki, E., Putaud, J. P., Balkanski, Y., Fuzzi, S., Horth, J., Moortgat, G. K., Winterhalter, R., Myhre, C. E. L., Tsigaridis, K., Vignati, E., Stephanou, E. G., and Wilson, J.: Organic aerosol and global climate modelling: a review, Atmos. Chem. Phys., 5, 1053–1123, doi:10.5194/acp-5-1053-2005, 2005.

Kroll, J. H. and Seinfeld, J. H.: Chemistry of secondary organic aerosol: formation and evolution of low-volatility organic in the atmosphere, Atmos. Environ., 42, 3593–3624, 2008.

Kroll, J. H., Smith, J. D., Che, D. L., Kessler, S. H., Worsnop, D. R., and Wilson, K. R.: Measurement of fragmentation and functionalization pathways in the heterogeneous oxidation of oxidized organic aerosol, Phys. Chem. Chem. Phys., 11, 8005–8014, doi:10.1039/B905289E, 2009.

Hygroscopicity, volatility and oxidation state of aerosol in the SE United States

K. M. Cerully et al.

Title Page

Abstract | Introduction

Conclusions | References

Tables | Figures

|◀ | ▶|

◀ | ▶

Back | Close

Full Screen / Esc

Printer-friendly Version

Interactive Discussion

Kroll, J. H., Donahue, N. M., Jimenez, J. L., Kessler, S. H., Canagaratna, M. R., Wilson, K. R., Altieri, K., E., Mazzoleni, L. R., Wozniak, A. S., Bluhm, H., Mysak, E. R., Smith, J. D., Kolb, C. E., and Worsnop, D. R.: Carbon oxidation state as a metric for describing the chemistry of atmospheric organic aerosol, Nature Chemistry, 3, 133–139, doi:10.1038/nchem.948, 2011.

Kuwata, M., Kondo, Y., Mochida, M., Takegawa, N., and Kawamura, K.: Dependence of CCN activity of less volatile particles on the amount of coating observed in Tokyo, J. Geophys. Res., 112, D11207, doi:10.1029/2006JD007758, 2007.

Lambe, A. T., Onasch, T. B., Massoli, P., Croasdale, D. R., Wright, J. P., Ahern, A. T., Williams, L. R., Worsnop, D. R., Brune, W. H., and Davidovits, P.: Laboratory studies of the chemical composition and cloud condensation nuclei (CCN) activity of secondary organic aerosol (SOA) and oxidized primary organic aerosol (OPOA), Atmos. Chem. Phys., 11, 8913–8928, doi:10.5194/acp-11-8913-2011, 2011.

Lance, S., Medina, J., Smith, J. N., and Nenes, A.: Mapping the operation of the DMT continuous flow CCN counter, Aerosol Sci. Tech., 40, 242–254, doi:10.1080/02786820500543290, 2006.

Lanz, V. A., Alfarra, M. R., Baltensperger, U., Buchmann, B., Hueglin, C., and Prévôt, A. S. H.: Source apportionment of submicron organic aerosols at an urban site by factor analytical modelling of aerosol mass spectra, Atmos. Chem. Phys., 7, 1503–1522, doi:10.5194/acp-7-1503-2007, 2007.

Lathem, T. L. and Nenes, A.: Water vapor depletion in the DMT continuous flow CCN chamber: effects on supersaturation and droplet growth, Aerosol Sci. Tech., 45, 604–615, doi:10.1080/02786826.2010.551146, 2011.

Lathem, T. L., Beyersdorf, A. J., Thornhill, K. L., Winstead, E. L., Cubison, M. J., Hecobian, A., Jimenez, J. L., Weber, R. J., Anderson, B. E., and Nenes, A.: Analysis of CCN activity of Arctic aerosol and Canadian biomass burning during summer 2008, Atmos. Chem. Phys., 13, 2735–2756, doi:10.5194/acp-13-2735-2013, 2013.

Li, Z., Schwier, A. N., Sareen, N., and McNeill, V. F.: Reactive processing of formaldehyde and acetaldehyde in aqueous aerosol mimics: surface tension depression and secondary organic products, Atmos. Chem. Phys., 11, 11617–11629, doi:10.5194/acp-11-11617-2011, 2011.

Li, Y.-H., Zhang, Z., Docherty, K.S., Zhang, H., Budisulistiorini, S. H., Rubitschun, C. L., Shaw, S. L., Knipping, E. M., Edgerton, E. S., Kleindienst, T. E., Gold, A., and Surratt, J. D.: Isoprene epoxydiols as precursors to secondary organic aerosol formation: acid-catalyzed

reactive uptake studies with authentic compounds, Environ. Sci. Technol., 46, 250–258, doi:10.1021/es202554c, 2012.

Massoli, P., Lambe, A. T., Ahern, A. T., Williams, L. R., Ehn, M., Mikkilä, J., Canagaratna, M. R., Brune, W. H., Onasch, T. B., Jayne, J. T., Petäjä, T., Kulmala, M., Laaksonen, A., Kolb, C. E., Davidovits, P., and Worsnop, D. R.: Relationship between aerosol oxidation level and hygroscopic properties of laboratory generated secondary organic aerosol (SOA) particles, Geophys. Res. Lett., 37, L24801, doi:10.1029/2010GL045258, 2010.

Meyer, N. K., Duplissy, J., Gysel, M., Metzger, A., Dommen, J., Weingartner, E., Alfarra, M. R., Prevot, A. S. H., Fletcher, C., Good, N., McFiggans, G., Jonsson, Å. M., Hallquist, M., Baltensperger, U., and Ristovski, Z. D.: Analysis of the hygroscopic and volatile properties of ammonium sulphate seeded and unseeded SOA particles, Atmos. Chem. Phys., 9, 721–732, doi:10.5194/acp-9-721-2009, 2009.

Moore, R. H. and Nenes, A.: Scanning flow CCN analysis – a method for fast measurements of CCN spectra, Aerosol Sci. Tech., 43, 1192–1207, doi:10.1080/02786820903289780, 2009.

Moore, R. H., Bahreini, R., Brock, C. A., Froyd, K. D., Cozic, J., Holloway, J. S., Middlebrook, A. M., Murphy, D. M., and Nenes, A.: Hygroscopicity and composition of Alaskan Arctic CCN during April 2008, Atmos. Chem. Phys., 11, 11807–11825, doi:10.5194/acp-11-11807-2011, 2011.

Nenes, A., Pilinis, C., and Pandis, S. N.: ISORROPIA: a new thermodynamic model for multiphase multicomponent inorganic aerosols, Aquat. Geochem., 4, 123–152, doi:10.1023/A:1009604003981, 1998.

Ng, N. L., Canagaratna, M. R., Zhang, Q., Jimenez, J. L., Tian, J., Ulbrich, I. M., Kroll, J. H., Docherty, K. S., Chhabra, P. S., Bahreini, R., Murphy, S. M., Seinfeld, J. H., Hildebrandt, L., Donahue, N. M., DeCarlo, P. F., Lanz, V. A., Prévôt, A. S. H., Dinar, E., Rudich, Y., and Worsnop, D. R.: Organic aerosol components observed in Northern Hemispheric datasets from Aerosol Mass Spectrometry, Atmos. Chem. Phys., 10, 4625–4641, doi:10.5194/acp-10-4625-2010, 2010.

Nguyen, T. B., Coggon, M. M., Bates, K. H., Zhang, X., Schwantes, R. H., Schilling, K. A., Loza, C. L., Flagan, R. C., Wennberg, P. O., and Seinfeld, J. H.: Organic aerosol formation from the reactive uptake of isoprene epoxydiols (IEPOX) onto non-acidified inorganic seeds, Atmos. Chem. Phys., 14, 3497–3510, doi:10.5194/acp-14-3497-2014, 2014.

Ohata, S., Moteki, N., and Kondo, Y.: Evaluation of a method for meaurement of the concentration and size distribution of black carbon particles suspended in rainwater, Aerosol Sci. Tech., 45, 1326–1336, 2011.

Orsini, D., Ma, Y., Sullivan, A., Sierau, B., Baumann, K., and Weber, R.: Refinements to the Particle-Into-Liquid Sampler (PILS) for ground and airborne measurements of water soluble aerosol composition, Atmos. Environ., 37, 1243–1259, 2003.

Padró, L. T., Tkacik, D., Lathem, T., Hennigan, C., Sullivan, A. P., Weber, R. J., Huey, L. G., and Nenes, A.: Investigation of cloud condensation nuclei properties and droplet growth kinetics of the water-soluble aerosol fraction in Mexico City, J. Geophys. Res., 115, D09204, doi:10.1029/2009JD013195, 2010.

Perry, R. H. and Green, D. W. (Eds.): Physical and chemical data, in: Perry's Chemical Engineers' Handbook, 7th edn., McGraw-Hill, New York, 1997.

Petters, M. D. and Kreidenweis, S. M.: A single parameter representation of hygroscopic growth and cloud condensation nucleus activity, Atmos. Chem. Phys., 7, 1961–1971, doi:10.5194/acp-7-1961-2007, 2007.

Petters, M. D., Wex, H., Carrico, C. M., Hallbauer, E., Massling, A., McMeeking, G. R., Poulain, L., Wu, Z., Kreidenweis, S. M., and Stratmann, F.: Towards closing the gap between hygroscopic growth and activation for secondary organic aerosol – Part 2: Theoretical approaches, Atmos. Chem. Phys., 9, 3999–4009, doi:10.5194/acp-9-3999-2009, 2009.

Portmann, R. W., Solomon, S., and Hegerl, G. C.: Spatial and seasonal patterns in climate change, temperatures, and precipitation across the United States, P. Natl. Acad. Sci. USA, 106, 7324–7329, 2009.

Poulain, L., Wu, Z., Petters, M. D., Wex, H., Hallbauer, E., Wehner, B., Massling, A., Kreidenweis, S. M., and Stratmann, F.: Towards closing the gap between hygroscopic growth and CCN activation for secondary organic aerosols – Part 3: Influence of the chemical composition on the hygroscopic properties and volatile fractions of aerosols, Atmos. Chem. Phys., 10, 3775–3785, doi:10.5194/acp-10-3775-2010, 2010.

Pye, H. O. T. and Seinfeld, J. H.: A global perspective on aerosol from low-volatility organic compounds, Atmos. Chem. Phys., 10, 4377–4401, doi:10.5194/acp-10-4377-2010, 2010.

Raatikainen, T., Lin, J. J, Cerully, K., Lathem, T. L., Moore, R. H., and Nenes, A.: CCN data interpretation under dynamic operation conditions, Aerosol Sci. Tech., 48, doi:10.1080/02786826.2014.899429, 2010

Title Page

Abstract | Introduction

Conclusions | References

Tables | Figures

|◀ | ▶|

◀ | ▶

Back | Close

Full Screen / Esc

Printer-friendly Version

Interactive Discussion

Reynolds, J. C., Last, D. J., McGillen, M., Nijs, A., Horn, A. B., Percival, C., Carpenter, L. J., and Lewis, A. C.: Structural analysis of oligomeric molecules formed from the reaction products of oleic acid ozonolysis, Environ. Sci. Technol., 40, 6674–6681, doi:10.1021/es060942p, 2006.

Roberts, G. and Nenes, A.: A continuous-flow streamwise thermal-gradient CCN chamber for atmospheric measurements, Aerosol Sci. Tech., 39, 206–221, doi:10.1080/027868290913988, 2005.

Ruehl, C. R., Chuang, P. Y., and Nenes, A.: Aerosol hygroscopicity at high (99 to 100 %) relative humidities, Atmos. Chem. Phys., 10, 1329–1344, doi:10.5194/acp-10-1329-2010, 2010.

Saleh, R., Shihadeh, A., and Khlystov, A.: On transport phenomena and equilibration time scales in thermodenuders, Atmos. Meas. Tech., 4, 571–581, doi:10.5194/amt-4-571-2011, 2011.

Sareen, N., Schwier, A. N., Shapiro, E. L., Mitroo, D., and McNeill, V. F.: Secondary organic material formed by methylglyoxal in aqueous aerosol mimics, Atmos. Chem. Phys., 10, 997–1016, doi:10.5194/acp-10-997-2010, 2010.

Tritscher, T., Dommen, J., DeCarlo, P. F., Gysel, M., Barmet, P. B., Praplan, A. P., Weingartner, E., Prévôt, A. S. H., Riipinen, I., Donahue, N. M., and Baltensperger, U.: Volatility and hygroscopicity of aging secondary organic aerosol in a smog chamber, Atmos. Chem. Phys., 11, 11477–11496, doi:10.5194/acp-11-11477-2011, 2011.

VanReken, T. M., Ng, N. L., Flagan, R. C., and Seinfeld, J. H.: Cloud condensation nucleus activation properties of biogenic secondary organic aerosol, J. Geophys. Res., 110, d07206, doi:10.1029/2004JD005465, 2005.

Varutbangkul, V., Brechtel, F. J., Bahreini, R., Ng, N. L., Keywood, M. D., Kroll, J. H., Flagan, R. C., Seinfeld, J. H., Lee, A., and Goldstein, A. H.: Hygroscopicity of secondary organic aerosols formed by oxidation of cycloalkenes, monoterpenes, sesquiterpenes, and related compounds, Atmos. Chem. Phys., 6, 2367–2388, doi:10.5194/acp-6-2367-2006, 2006.

Villani, P., Sellegri, K., Monier, M., and Laj, P.: Influence of semi-volatile species on particle hygroscopic growth, Atmos. Environ., 79, 129–173, 2013.

Wang, S. C. and Flagan, R. C.: Scanning electrical mobility spectrometer, Aerosol Sci. Tech., 13, 230–240, 1990.

Weber, R. J., Orsini, D., Daun, Y., Lee, Y.-N., Klotz, P., and Brechtel, F.: A particle-into-liquid collector for rapid measurements of aerosol chemical composition, Aerosol Sci. Tech., 35, 718–727, 2001.

Title Page

Abstract | Introduction

Conclusions | References

Tables | Figures

|◄ | ►|

◄ | ►

Back | Close

Full Screen / Esc

Printer-friendly Version

Interactive Discussion

Wex, H., Petters, M. D., Carrico, C. M., Hallbauer, E., Massling, A., McMeeking, G. R., Poulain, L., Wu, Z., Kreidenweis, S. M., and Stratmann, F.: Towards closing the gap between hygroscopic growth and activation for secondary organic aerosol: Part 1 – Evidence from measurements, Atmos. Chem. Phys., 9, 3987–3997, doi:10.5194/acp-9-3987-2009, 2009.

Xu, L., Guo, H., Boyd, C. M., Klein, M., Bougiatioti, A., Cerully, K. M., Hite, J. R., Isaacman-VanWerts, G., Kreisberg, N. M., Knote, C., Olson, K., Koss, A., Goldstein, A. H., Hering, S. V., de Gouw, J., Baumann, K., Lee, S.-H., Nenes, A., Weber, R. J., and Ng, N. L.: Effects of anthropogenic emissions on aerosol formation from isoprene and monoterpenes in the Southeastern United States, P. Natl. Acad. Sci. USA, in review, 2014a.

Xu, L., Kollman, M. S., Song, C., Shilling, J. E., and Ng, N. L.: Effects of NO_x on the volatility of secondary organic aerosol from isoprene photooxidation, Environ. Sci. Technol., 48, 253–2262, 2014b.

Zuend, A. and Seinfeld, J. H.: Modeling the gas-particle partitioning of secondary organic aerosol: the importance of liquid-liquid phase separation, Atmos. Chem. Phys., 12, 3857–3882, doi:10.5194/acp-12-3857-2012, 2012.

Title Page

Abstract | Introduction

Conclusions | References

Tables | Figures

|◄ | ►|

◄ | ►

Back | Close

Full Screen / Esc

Printer-friendly Version

Interactive Discussion

Table 1. Average and SD in κ of non-denuded and thermally-denuded ambient and water-soluble ambient aerosol.

s (%)	Ambient			PILS		
	0.40	0.30	0.20	0.40	0.30	0.20
Non-denuded	0.18 ± 0.05	0.21 ± 0.05	0.25 ± 0.08	0.25 ± 0.06	0.25 ± 0.07	0.23 ± 0.09
TD at 60 °C	0.17 ± 0.05	0.20 ± 0.06	0.24 ± 0.08	0.26 ± 0.07	0.26 ± 0.08	0.25 ± 0.09
TD at 80 °C	0.19 ± 0.08	0.22 ± 0.10	0.25 ± 0.10	0.26 ± 0.06	0.27 ± 0.07	0.27 ± 0.12
TD at 100 °C	0.19 ± 0.04	0.23 ± 0.04	0.30 ± 0.05	0.31 ± 0.10	0.27 ± 0.10	0.31 ± 0.13

Table 2. Average and SD in MFR and relative change of thermally-denuded vs. non-denuded aerosol for ambient κ measured at $s = 0.20\%$ and PILS κ measured at $s = 0.40\%$.

	Ambient		PILS	
	MFR	$\frac{\kappa_{TD} - \kappa_{o}}{\kappa_{o}}$	MFR	$\frac{\kappa_{TD} - \kappa_{o}}{\kappa_{o}}$
TD at 60 °C	0.90 ± 0.10	-0.02 ± 0.20	0.73 ± 0.19	0.01 ± 0.12
TD at 80 °C	0.78 ± 0.05	0.11 ± 0.33	0.65 ± 0.11	0.10 ± 0.10
TD at 100 °C	0.65 ± 0.08	0.12 ± 0.16	0.45 ± 0.13	0.11 ± 0.07

Table 3. Average and SD in κ_{org} of non-denuded and denuded ambient aerosol at $s = 0.20\%$ and water-soluble ambient aerosol at $s = 0.40\%$ using bulk AMS composition and PILS-IC with ISORROPIA II composition.

| | AMS | | PILS-IC |
	Ambient ($s = 0.20\%$)	PILS ($s = 0.40\%$)	PILS ($s = 0.40\%$)
Non-denuded	0.14 ± 0.09	0.14 ± 0.06	0.11 ± 0.07
TD at 60 °C	0.12 ± 0.08	0.12 ± 0.06	–
TD at 80 °C	0.12 ± 0.11	0.09 ± 0.04	–
TD at 100 °C	0.08 ± 0.07	0.08 ± 0.06	–
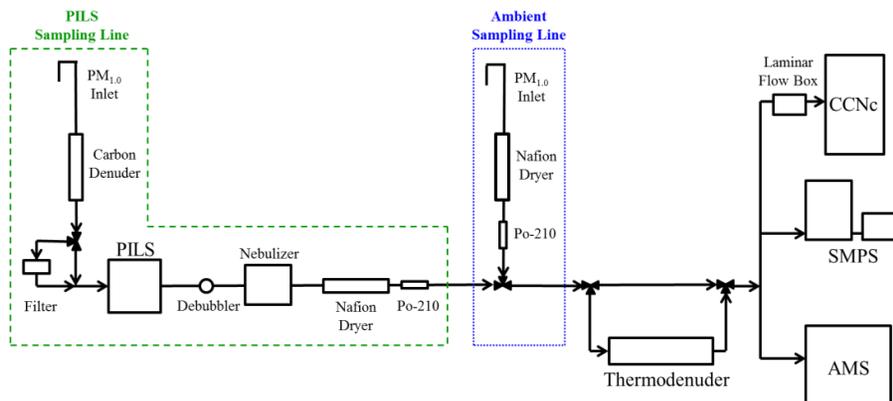
Figure 1. Instrument setup used during the SOAS campaign, combining a PILS, thermodenuder, CCNc, AMS, and SMPS to measure the water-soluble fraction of ambient aerosol (green dashed line) and ambient aerosol (blue dotted line).
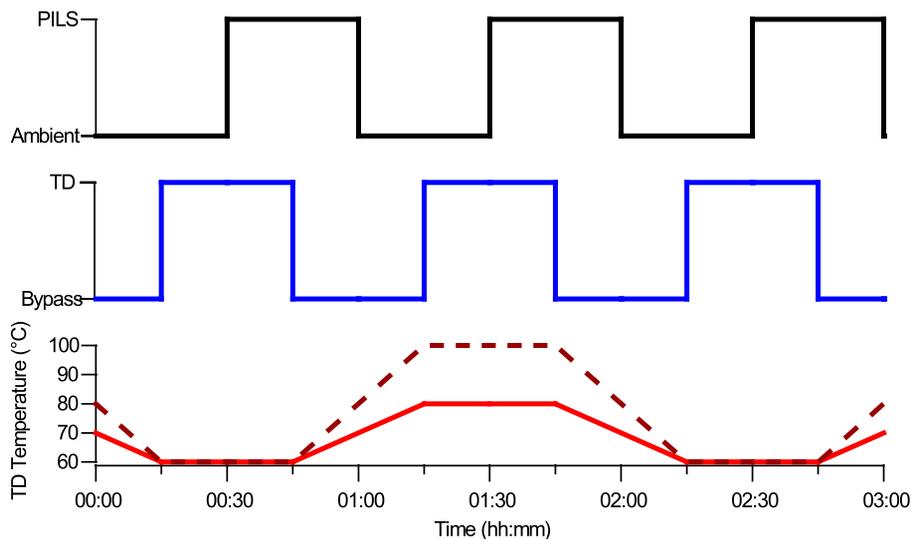
Figure 2. Example sampling schedule illustrating the valve switching between both PILS and ambient sampling lines and TD and bypass sampling lines. TD sampling temperatures from 20 June to midday 30 June are indicated by the red, solid line, and sampling temperatures from evening 30 June to 15 July are indicated by the dashed line.
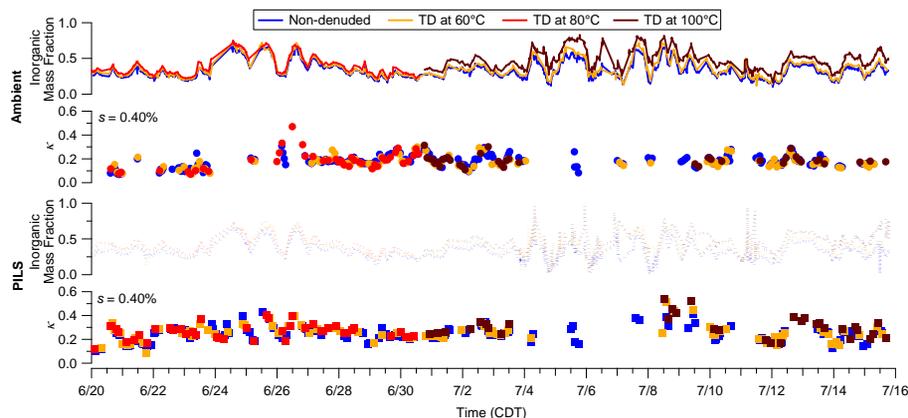
Figure 3. Temporal ambient (top) and PILS (bottom) κ and AMS inorganic mass fractions for the entire study. Non-denuded and thermally-denuded measurements are indicated by color. Each point represents an average of all κ values measured over each 15 min sampling period.
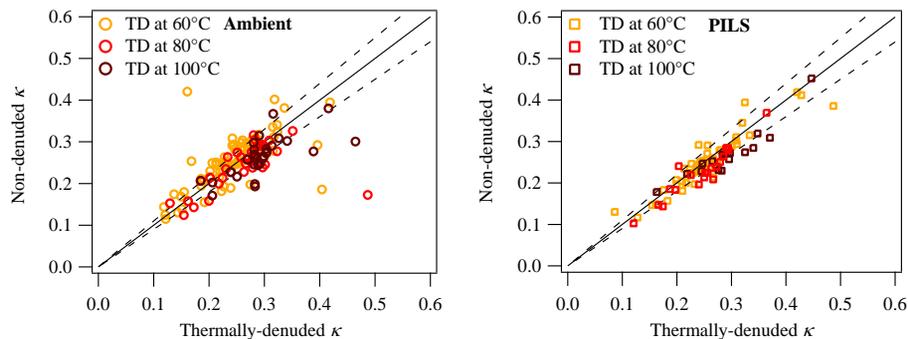
Figure 4. Non-denuded vs. thermally-denuded κ at 60, 80, and 100 °C TD sampling temperatures for ambient aerosol at $s = 0.20\%$ (left) and PILS aerosol at $s = 0.40\%$ (right). The solid line represents 1 : 1 agreement while dashed lines represent deviations of ±10 %. All points shown are for periods where non-denuded measurements are directly followed by denuded measurements and vice versa.
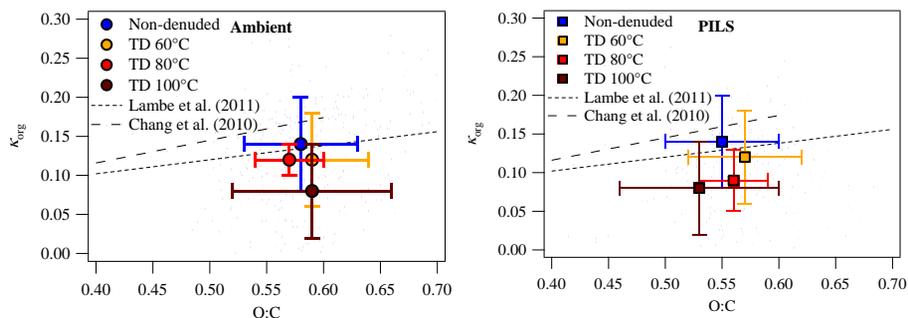
Figure 5. Variation in κ_{org} with O : C for ambient aerosol at $s = 0.20\,\%$ and PILS aerosol at $s = 0.40\,\%$ for non-denuded and thermally-denuded conditions. Small colored dots indicate all measured points while larger circles and squares indicate the averages for while errors bars indicate one SD in measured values for ambient and PILS aerosol, respectively. Also shown are dashed lines indicating the parameterizations of κ_{org} with O : C from Lambe et al. (2011) and Chang et al. (2010).
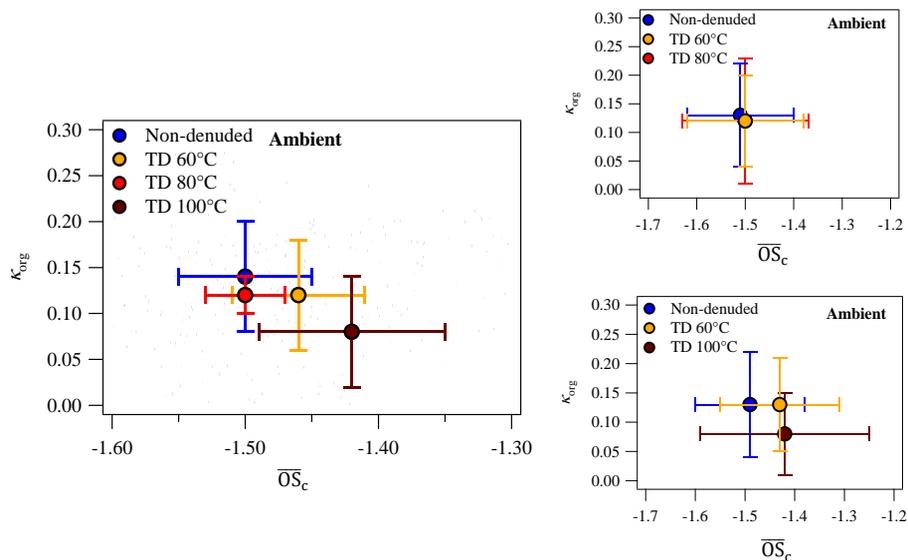
Figure 6. Variation in κ_{org} with $\overline{OS}_c$ for ambient aerosol at $s = 0.20\,\%$ for the total study period (left) and for 80 and 100 °C measurement periods only (right top and bottom, respectively). Small colored dots indicate all measured points while larger circles indicate measurement averages and errors bars indicate a single SD in measured values.
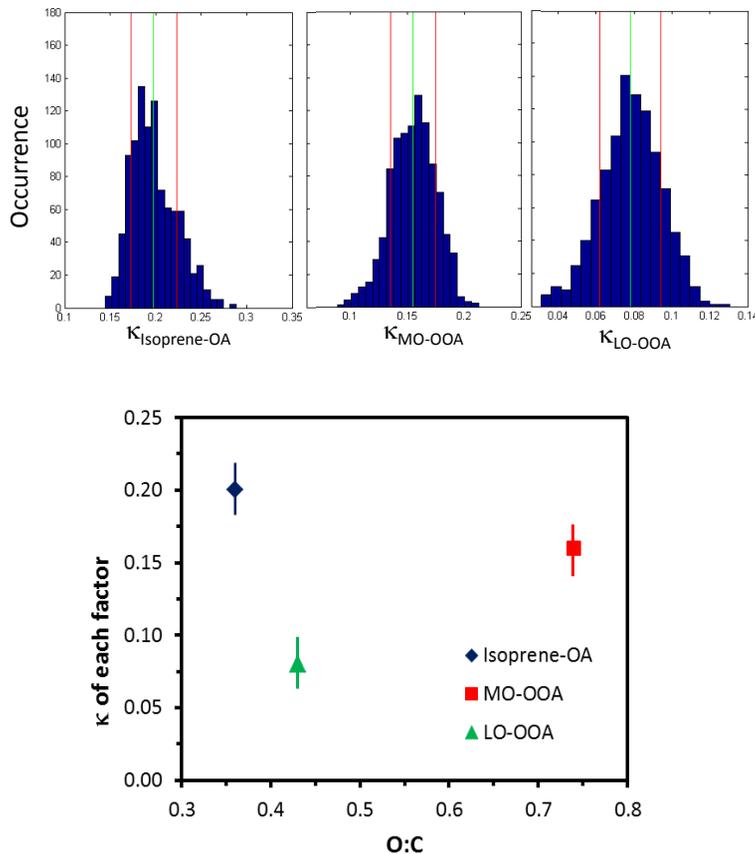
Figure 7. (top panels) Examples of binned κ_{or} solutions from a bootstrapped resampling of the linear regression of the CCN activity of PILS bypass aerosol, where the solid green and red lines represent the average and one SD, respectively in each factor. (bottom panel) κ_{or} found for each PMF factor through linear regression vs. O : C for non-denuded PILS aerosol at $s = 0.40\,\%$, where error bars represent the SD obtained from the bootstrap analysis.

Title Page

Abstract | Introduction

Conclusions | References

Tables | Figures

|◄ | ►|

◄ | ►

Back | Close

Full Screen / Esc

Printer-friendly Version

Interactive Discussion
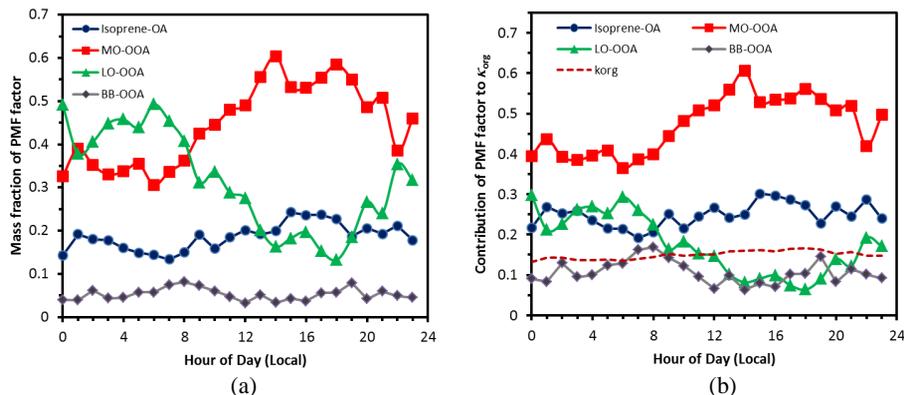
Figure 8. (a) Average mass fraction diurnal profile of the three characteristic aerosol factors identified in the AMS spectra. **(b)** The corresponding diurnal contribution of each aerosol factor to the κ_{org}, computed by multiplying the mass fraction by the corresponding hygroscopicity parameter (Fig. 7), and the predicted diurnal profile of the total κ_{or} in the ambient aerosol.